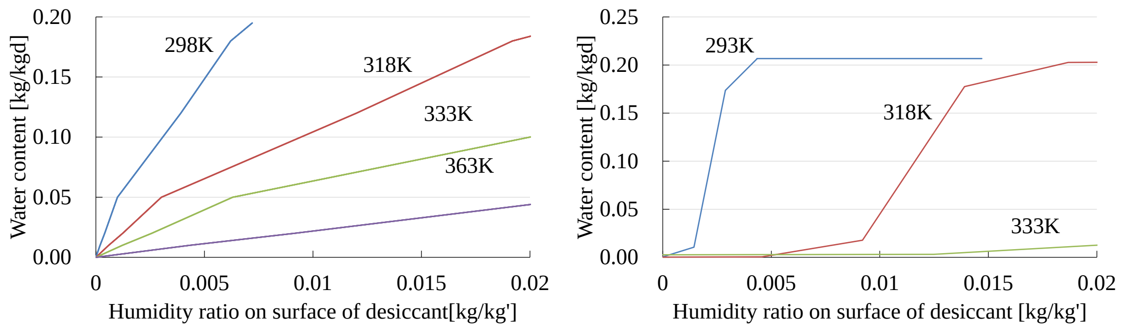

(a) ***Silica gel*** **(b)** ***zeolite***

Figure 3. *Adsorption isotherm of each material*

Table 1. *Approximation of the adsorption isotherm of silica gel*

Temperature of desiccant plate	Approximation
298 K	$X_b = 0.0348w^*$
318 K	$X_b = 0.1074w^*$
333 K	$X_b = 0.2306w^*$
363 K	$X_b = 0.9771w^*$

Table 2. *Approximation of the adsorption isotherm of zeolite*

Temperature of desiccant plate	Approximation
298 K	$X_b = 0.1434w^* - 7E\text{-}05$ ($w^* < 0.0105$) $X_b = 0.0129w^* + 0.0012$ ($w^* < 0.2063$) $X_b = 3E\text{-}07w^* + 0.0043$ ($w^* \geqq 0.2063$)
318 K	$X_b = 0.3989w^* + 0.0021$ ($w^* < 0.0178$) $X_b = 0.058w^* + 0.0076$ ($w^* < 0.2031$) $X_b = 0.183w^* - 0.0136$ ($w^* \geqq 0.2031$)
338 K	$X_b = 1.1705w^* + 0.0027$ ($w^* < 0.0195$) $X_b = 0.1431w^* + 0.0216$ ($w^* < 0.1945$) $X_b = 1.5956w^* - 0.2513$ ($w^* \geqq 0.1945$)

System Parameter study Conditions

Many parameters affect desiccant system’s performance. Several important factors are selected based on the rotor type desiccant system study by Yamaguchi (2010):

- Air flow rate through the system
- Thickness of the desiccant plate
- Sectional area of the desiccant plate

・Switching period of the desiccant plate
・Number of stages (desiccant plates in a line)

These factors are evaluated by numerical model simulations. The boundary conditions for the parameter study are showed in Table 3. The average air state in summer in Japan is adopted as the outside air condition. The cold water is assumed to be obtained from the cooling tower, and the hot water is assumed to be cogenerated. Table 4 shows the cases of the parameter study. The underlined values are the standard values of each parameter.

Table 3. *Boundary conditions of the numerical simulations*

Outside air	32 ℃, 0.0185 kg/kg'(55%RH)
Return air	28 ℃, 0.013 kg/kg'(48%RH)
Cold water of heat exchanger	26 ℃, 0.1 kg/s
Hot water of heat exchanger	60 ℃, 0.1 kg/s
Desiccant material	Zeolite

Table 4. *Study cases*

Air flow rate through system	250 , 500 , 1000 m^3/h
Sectional area of desiccant plate	0.02 , 0.05 , 0.1 , 0.15 , 0.20 m^2
Thickness of desiccant plate	0.02 , 0.05 , 0.10 , 0.15, 0.20 m
Switching period of desiccant plate	0 - 3600 s
Number of stages	1 - 3

RESULTS

Fig.4 shows the results of the system performance as change of the air flow rate. It shows the dehumidification amount in 3,600 s for each air flow rate. With larger air flow, the total dehumidification performance is reduced, because the relative humidity of the outlet air from the cooling coil was lower. Fig.5 shows the results of the study of the sectional area of the plate. It shows the dehumidification in 3,600 s versus the sectional area (Fig.5(a)) and the dehumidification per sectional area versus the air velocity (Fig.5(b)). This indicates that when the sectional area of the plate is constant, the dehumidification was higher as air velocity is faster. Fig.6 shows the dehumidification amount in 3600 s versus desiccant plate thickness. When the plate was thicker, dehumidification was higher. A thick desiccant plate can dehumidify the air moisture by a large amount of desiccant material and performance is therefore better. Fig.7 shows the investigation of the switching period of the plates. This graph shows that an optimum switching period existed.

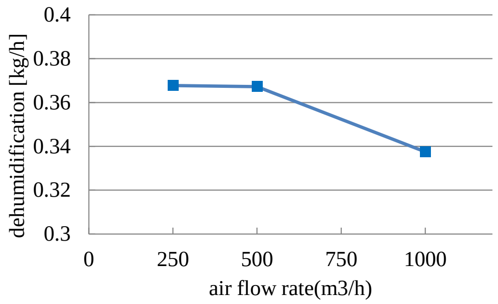

Figure 4. *The results of dehumidification performance as air flow rate and air velocity*

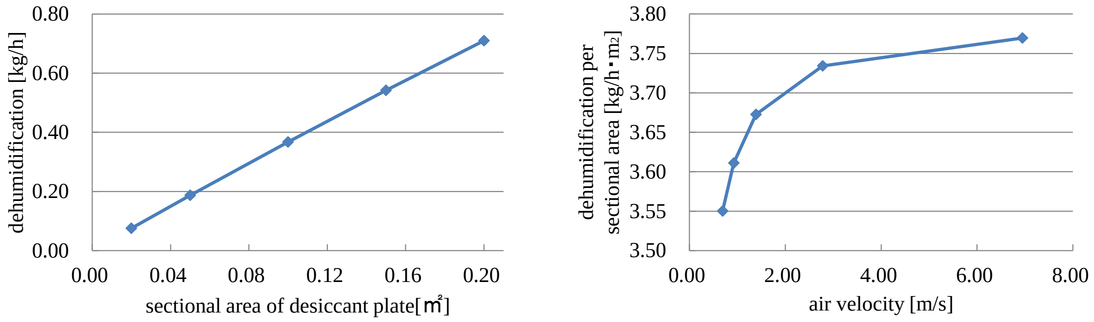

(a) *sectional area of desiccant plate* (b) *air velocity*

Figure 5. *The results of dehumidification with the relation sectional area of desiccant plate and air velocity*

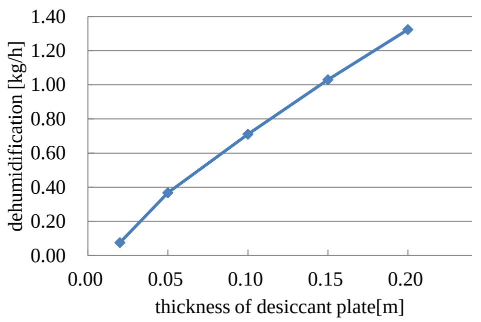

Figure 6. *The effect of dehumidification performance by thickness of desiccant plate*

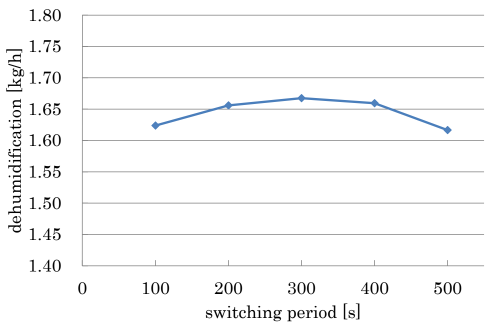

Figure 7. *The effect of dehumidification performance by switching period*

Multiplate system Study

The parameter studies showed the basic effect of each parameter, but effect when each parameter varies simultaneously needs to be discussed. Fig.8 shows the correlation between the optimum switching period and the dehumidification performance per area of plate against air velocity for two plate thicknesses. The optimal switching period was the period the best dehumidification. When the air velocity is faster, the optimal switching period is shorter. This means that much air flow can be processed in a short time.

The system had limited potential with a single desiccant plate, but its performance could be improved by combining several plates in a line. Fig.9 shows the results of simulations of single to triple stage plate desiccant systems. This indicates that multiplate systems improved performance without raising the hot water temperature.

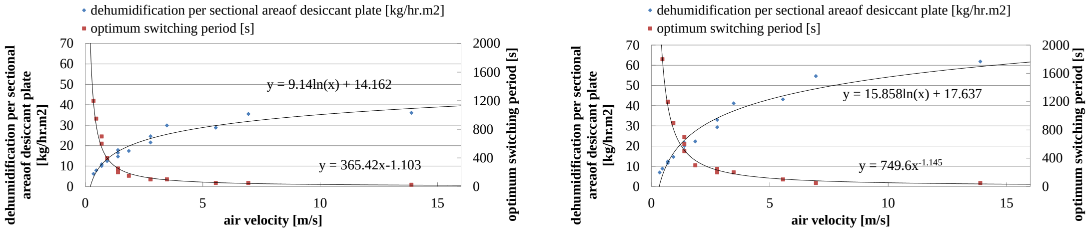

(a) Thickness of desiccant plate 0.05m (b) Thickness of desiccant plate 0.10m

Figure 8. The result of parameter studies

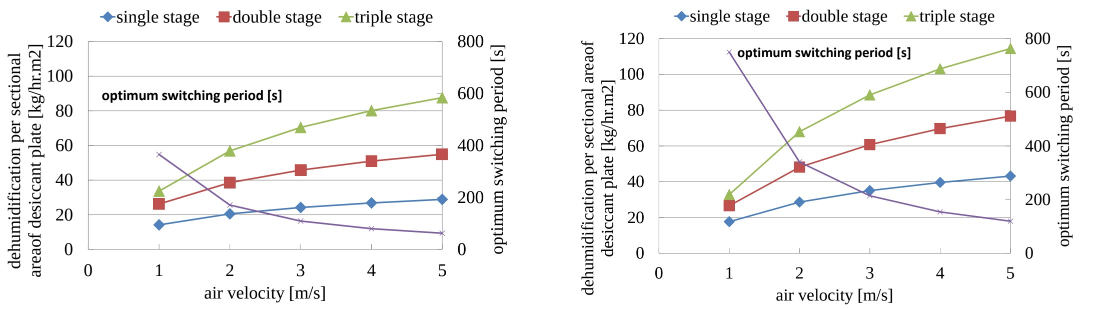

(a)Thickness of desiccant plate 0.05m (b)Thickness of desiccant plate 0.10m

Figure 9. *The integrated dehumidification performance diagram*

CONCLUSION

A numerical model of the plate type desiccant system has been proposed, and performance analysis was conducted assuming that cold water was obtained from a cooling tower and hot water was cogenerated. A parameter study defined the effect of each parameter on dehumidification performance. All results were integrated in the dehumidification performance diagram (Fig.9). This diagram can be used as reference for system design. For example, the thickness and area of the desiccant plate, the switching period, and number of stages that achieve required dehumidification performance can be designed.

The pressure drop and heat distribution on the surface of the desiccant plate, etc., should be investigated in future. Model experiments should be conducted to build a more precise numerical model. Furthermore, a feasibility study has to be conducted with the numerical model. It is important to study from the point of view of air process performance and energy consumption.

ACKNOWLEDGEMENTS

This work was supported by JSPS KAKENHI Grant Number 26820249.

REFERENCES

Rang, T., Xiao-Hua, L. and Yi. J. 2013. Performance analysis of a new kind of heat pump-driven outdoor air processor using solid desiccant, Renewable Energy 57, pp101-110

Momoi, Y., Yoshie, R., Satake, A., Yoshino, H. 2006. Numerical Simulation of Moisture Adsorption-Desorption for Desiccant Dehumidifier, Part 4 Calculation Dehumidification Coefficient of Desiccant Rotor, Proceedings of the Society of Heating, Air-Conditioning and Sanitary Engineers of Japan 2006.

Yamaguchi, S. 2010. Numerical and Experimental Performance Evaluation for Silica Gel Desiccant Wheel, Waseda University (Japan).

Symbols

t	Time [s]
ε	Prorosity of porous solid [-]
C_a	Specific heat at constant pressure of air [J/kg・K]
C_d	Specific heat of desiccant [J/kg・K]
ρ_a	Density of humid air [kg/m^3]
ρ_d	Density of desiccant [kg/m^3]
α	Heat diffusivity [W/m^{2}K]
α'	Mass diffusivity [kg/m2 s kg/kg(DA)]
S_d	Surface area per volume [m^2/m^3]
L	Latent heat [J/kg]
T_a	Temperature of air [℃]
T_d	Temperature of desiccant [℃]
X_a	Absolute humidity ratio of air [kg/kg(DA)]
X_b	Absolute humidity of surface of desiccant [kg/kg(DA)]
W	Water content of desiccant [kg/kg$_d$]
W^*	Water content at equilibrium of desiccant [kg/kg$_d$]
u	Velocity of air [m/s]
$_{ave}$	Average value in the cell